

Indirect imaging of the accretion stream in HU Aquarii

M.K. Harrop-Allin and M. Cropper

*Mullard Space Science Laboratory, University College London,
Holmbury St. Mary, Dorking, Surrey, RH5 6NT, UK*

P.J. Hakala

Observatory and Astrophysics Laboratory, Univ. of Helsinki, Finland

C. Hellier

Department of Physics, Keele University, Staffordshire, UK

T. Ramseyer

Dept. of Physics and Astronomy, Univ. of Central Arkansas, USA

Abstract. We apply our technique for indirect imaging of the accretion stream to *UBVR* eclipse profiles of HU Aqr obtained when the system was in a high state. We perform model fits to the eclipses using two geometries: one where the stream accretes onto one footpoint of the field line, and the other where the stream accretes onto both footpoints. We find that the stream brightness is not uniform, nor is it a simple function of the radial distance from the white dwarf. The model provides estimates of the radius where the stream couples to the magnetic field ($1.0 - 1.3 \times 10^{10}$ cm) and of the mass transfer rate ($8 - 76 \times 10^{16}$ g/s). We examine the wavelength dependence of the stream brightness, and find that in the case of the two-footpoint model, the sections of the magnetically-constrained stream immediately adjacent to the coupling radius appear to be hotter than the remainder of the stream. This may be due to shock heating of the plasma as it threads onto the magnetic field.

1. Scientific context

The mechanisms whereby the accretion stream in polars becomes coupled to the magnetic field are complex and not well-understood. In order to provide further observational constraints to this problem, we have developed a method to image the accretion stream in eclipsing polars. The technique has close parallels with eclipse mapping of accretion discs in non-magnetic systems (e.g. Marsh & Horne 1988), in that both use photometric eclipse profiles to deduce the distribution of emission between the component stars, and both make use of maximum entropy regularization to constrain the problem. Our method operates by placing emission points along a pre-set stream trajectory, and then “observing” the model

stream through an eclipse by a Roche lobe-filling secondary star. The relative brightnesses of the emission points are adjusted to obtain the most locally smooth stream whose eclipse profile matches an observed profile. The optimization is performed using a Genetic Algorithm in order to maximize our chances of finding the global optimum in the multi-dimensional space. For more details and tests of the method, see Harrop-Allin, Hakala & Cropper (1998). We present here the results of applying this method to HU Aqr observed in a high accretion state ($V \sim 15.1$).

The data used for the modelling were obtained in August 1993 using the Stiening photometer on the 2.1 m reflector at McDonald Observatory. The imaging procedure was applied to a total of five eclipses obtained over three consecutive nights. The eclipse profiles are asymmetrical and show two chief components: a steep component due to the accretion region on the white dwarf, and a more gradual component due to the accretion stream. The stream's contribution to the total emission is comparable, and in U and B *exceeds*, the emission from the accretion region. There are prominent pre-eclipse absorption dips at orbital phase $\phi \sim 0.88$ in all four wavebands in the high state. The phase of the dip centre moves to successively earlier phases during the course of the observations (which cover three nights), implying an increase in the angle between the absorbing material and the line of centres from 42° to 48° . This dramatic movement of the stream occurs without any change in the overall brightness of the system.

2. The stream brightness distributions

Before the imaging procedure can be applied, a choice has to be made whether to use a model stream that accretes at one pole or both. HU Aqr shows evidence for both one and two-pole accretion in the high state. On one hand, the overall shape of the light curve is consistent with cyclotron beaming from a single pole. On the other hand, circular polarimetry obtained in June 1993 when the system was also in a high state (Hakala, unpublished data) shows clear positive and negative excursions, suggesting accretion onto (at least) two regions of the opposite polarity. We therefore perform model fits to the eclipse profiles using both geometries, and present sample results of each.

Figure 1 shows sample results for the two-footpoint geometry model. Good fits to all five cycles were obtained using an orbital inclination of 85° and a mass ratio of 0.25. The ballistic stream is diverted by the magnetic field at a radius R_μ in the range $0.21 a \lesssim R_\mu \lesssim 0.23 a$ (where a is the orbital separation of the two stars). The magnetic colatitude β of the dipole field is in the range $22^\circ \lesssim \beta \lesssim 27^\circ$ and its longitude ζ is 10° (this latter value is not well-constrained by the model; equally good fits were obtained for values in the range 0 – 30°). There are no obvious trends in β or R_μ over the three nights.

The stream images show that the brightness is not uniform along the stream, nor is it a simple function of the radial distance from the white dwarf. Rather, there are regions of the stream with localized brightness enhancements, particularly within the magnetosphere. Interestingly, there is no obvious brightening of the stream as it approaches either the threading radius or the white dwarf.

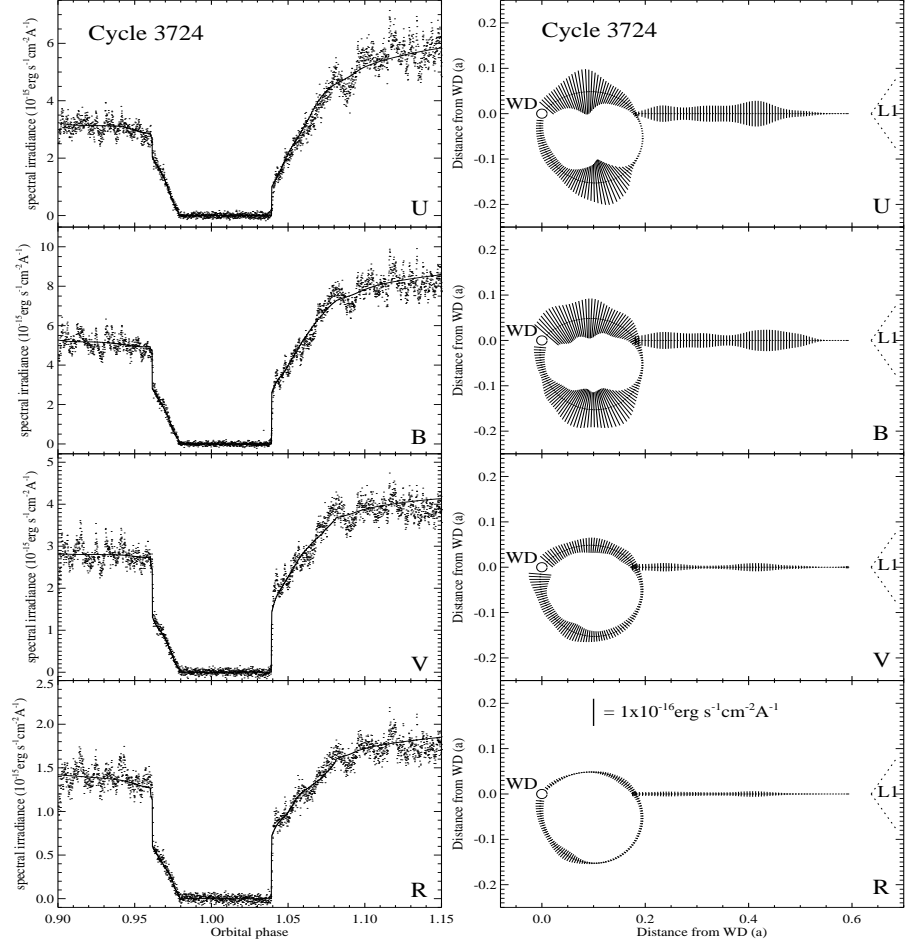


Figure 1. Model eclipse profiles and the corresponding images of the accretion stream for cycle 3724 (according to the ephemeris in Schwöpe, Mantel & Horne 1997), using a stream that accretes onto both foot-points of a dipole field line. The stream images are shown projected onto the plane perpendicular to the orbital plane and passing through the centre of both stars. The brightness of each emission point is shown as a line through the point, perpendicular to the stream; the length of each line indicates the brightness of the point. The white dwarf is shown to scale as a circle (labelled ‘WD’), and the secondary is shown (not to scale) to mark the position of the L1 point (labelled ‘L1’).

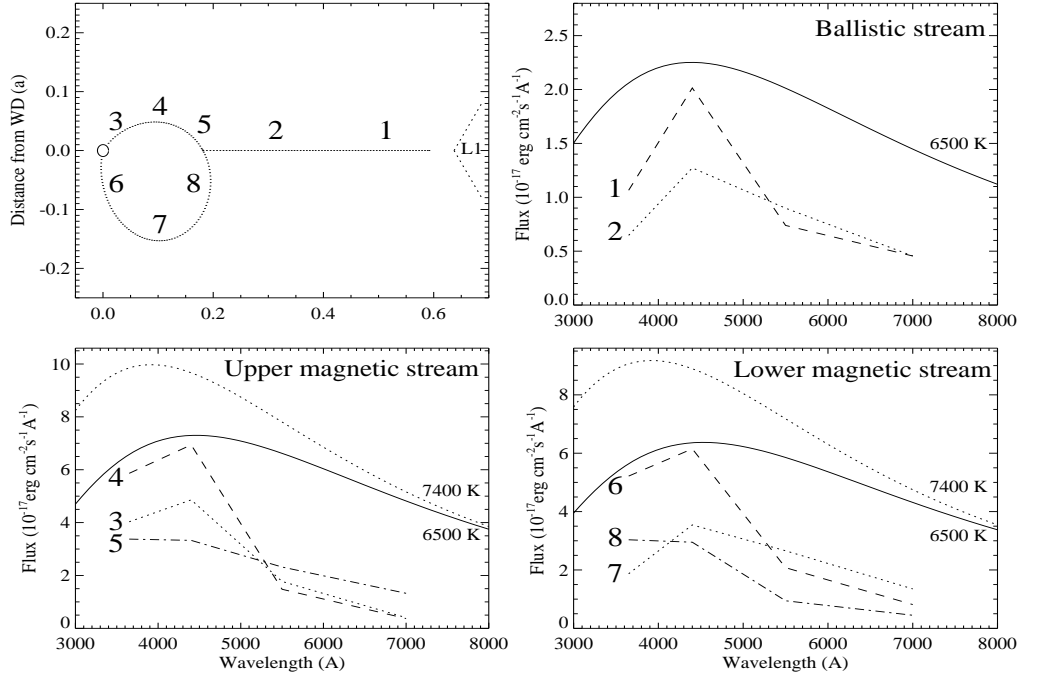


Figure 2. The colour-dependence of the stream brightness distributions for cycle 3723 (similar results are found for the other four cycles). The stream is divided into eight sections (top left panel) and the average flux per stream emission point in each section is plotted in the four wavebands for each of the eight sections of the stream. Note the comparable U and B fluxes in sections 5 and 8. Blackbody curves for temperatures of 6500 K and 7400 K are shown for illustration.

To investigate the wavelength dependence of the stream images, the stream is divided into eight sections and the average flux per stream emission point in each section is examined in turn. In all stream sections apart from sections ‘5’ and ‘8’ (see Fig. 2), and in all cycles, the stream flux is highest in B and successively lower in U , V and R . In four of the five cycles, the stream flux is comparable in U and B in sections ‘5’ and ‘8’.

Fig. 3 shows the results for the same eclipse profile as in Fig. 1, but modelled using a stream that accretes onto only the pole on the same side of the orbital plane as the observer. The one-footpoint model fits were obtained using $\beta = 30^\circ$ and $\zeta = 10^\circ$ (once again ζ is not well-constrained). The coupling radius decreases from $0.20 a$ to $0.17 a$ over the three nights. This results in an increase in the angle between the magnetically-channeled part of the stream and the line of centres, from 42° to 47° . Interestingly, this is almost identical to the range of angles implied by the movement of the pre-eclipse dip.

The stream images are quite different from the two-footpoint geometry results. There is very little emission from the ballistic stream. The stream brightens as it approaches R_μ . As the stream leaves the orbital plane it fades, and

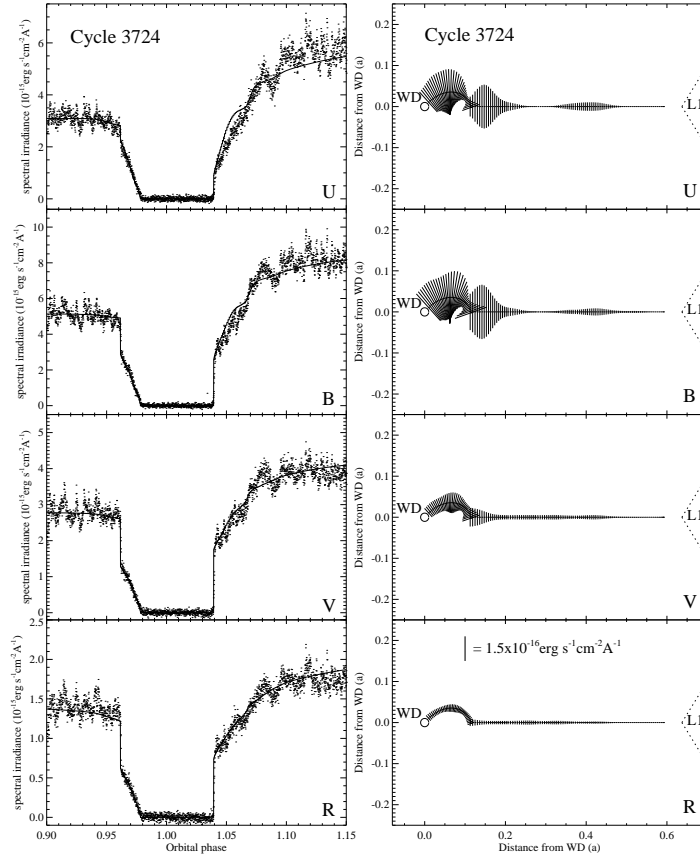


Figure 3. As for Fig. 1, but for a model stream that accretes onto only the footpoint of the field line above the orbital plane (on the same side of the orbital plane as the observer).

then brightens again as it approaches the white dwarf. The brightest part of the stream is not always closest to the white dwarf, though: in several cycles the peak emission occurs about $0.08 a$ from the surface.

We examine the wavelength dependence of the stream brightness as before by dividing the stream into sections. For this geometry we divided both the ballistic and the magnetically-channeled part of the stream into two sections. In all cycles and all stream sections (without exception) the flux is highest in B , and is successively lower in U , V and R .

3. What can be deduced about the accretion stream?

The range of values obtained for the coupling radius is $1.0\text{--}1.3 \times 10^{10}$ cm, or 17–21 white dwarf radii. The radius of the stream can be estimated using the pre-eclipse absorption dips; we find a radius of 3×10^9 cm. If we make the canonical assumption that the ram pressure of the stream is balanced by the magnetic pressure at R_μ , we can estimate the mass transfer rate in the stream: this is found to be $8\text{--}76 \times 10^{16} \text{ g s}^{-1}$. The smaller values in this range are in agreement with the mass transfer rate obtained by Heerlein, Horne & Schwöpe (1998) from their models of the accretion flow in HU Aqr.

What emission mechanisms are operating in the stream to provide sufficient optical flux to rival the flux from the accretion region? The stream flux is not likely to be cyclotron emission due to its low levels of polarization (this is can

be seen from simultaneous intensity and polarization light curves). Also, the cyclotron emission would be strongest where the thermal velocity of electrons is highest. The bulk of the cyclotron radiation is thus expected to be radiated from the post-shock flow close to the white dwarf surface, and is unlikely to be the origin of the emission many white dwarf radii from the white dwarf surface.

We can also eliminate line emission as the chief emission mechanism. This is because line emission is strongest in the ballistic stream (as seen in contemporaneous Doppler tomograms: Schwobe et al. 1997), whereas the *total* line and continuum emission (as seen in the stream images) is greatest in the magnetosphere. Free-free emission, although providing sufficient flux, does not have the correct spectral shape to match the wavelength dependence of the stream.

As shown in Fig. 2, the stream fluxes in *UBVR* are closer to blackbody spectra. They do not match a blackbody curve exactly, deviating in the *U* and *R* fluxes which fall significantly below a blackbody curve. However, the stream fluxes in the various sections of the stream peak in *B* in most cases, and this is roughly consistent with a blackbody of temperature 6500 K. The exceptions to this occur in the case of the two-footpoint geometry models, where the stream sections on the magnetic part of the stream immediately adjacent to R_μ have *U* fluxes comparable to *B*. This suggests that the stream plasma that has just been threaded is hotter than the fully-threaded plasma closer to the white dwarf and than the free-falling plasma before the threading radius. This may be due to shock heating of the plasma as it threads onto the magnetic field, as suggested by e.g. Liebert & Stockman (1985) and Hameury, King & Lasota (1986).

References

- Harrop-Allin M.K., Hakala P.J., Cropper M., 1998, MNRAS, in press
 Heerlein C., Horne K., Schwobe A.D., 1998, MNRAS, in press
 Hameury J.-M., King A.R., Lasota J.-P., 1986, MNRAS, 218, 695
 Liebert J., Stockman H.S., 1985, in Lamb D.Q., Patterson J., eds, Cataclysmic Variables and Low-Mass X-ray Binaries. Reidl, Dordrecht, p. 151
 Schwobe A.D., Mantel K.-H., Horne K., 1997, A&A, 319, 894